

Spin-Transition Polymers: From Molecular Materials Toward Memory Devices

O. Kahn* and C. Jay Martinez

Some $3d^n$ ($4 \leq n \leq 7$) transition metal compounds exhibit a cooperative transition between a low-spin (LS) and a high-spin (HS) state. This transition is abrupt and occurs with a thermal hysteresis, which confers a memory effect on the system. The intersite interactions and thus the cooperativity are magnified in polymeric compounds such as $[\text{Fe}(\text{Rtrz})_3]\text{A}_2 \cdot n\text{H}_2\text{O}$ in which the Fe^{2+} ions are triply bridged by 4-R-substituted-1,2,4-triazole molecules. Moreover, in these compounds, the spin transition is accompanied by a well-pronounced change of color between violet in the LS state and white in the HS state. The transition temperatures of these materials can be fine tuned, using an approach based on the concept of a molecular alloy. In particular, it is possible to design a compound for which room temperature falls in the middle of the thermal hysteresis loop. These materials have many potential applications, for example, as temperature sensors, as active elements of various types of displays, and in information storage and retrieval.

The use of molecules or molecular assemblies for information processing is one of the most appealing perspectives in molecular chemistry. Whatever the final goal, a fundamental underlying concept is that of molecular bistability (1), which may be defined as the ability of a molecular system to be observed in two different electronic states in a certain range of external perturbation. Usually, one of the states is the ground state, and the other is a metastable state. Molecular bistability may refer to either a single molecule or to an assembly of molecules. To be used in memory devices, the bistability must be associated with a response function, for instance, optical or magnetic, which reveals the state of the system.

One of the most spectacular examples of molecular bistability is the spin-crossover phenomenon. It was first observed in 1931 (2, 3) and has been investigated extensively since the mid-1970s (4-9). Only during the 1980s, however, was it realized that spin-crossover compounds could be used as active elements in memory devices (10-14). In 1984, it was found that a green light switches the LS state to the HS one, which has practically infinitely long lifetimes below 50 K, and that a red light switches the system back from the HS state to the LS state (14-16). The discovery of this LIESST (light-induced excited spin-state trapping) effect suggested that the spin-crossover compounds could be used as optical switches.

Let us briefly explain the essence of the spin-crossover phenomenon. Some molecular species containing an octahedrally coordinated transition metal ion with the $3d^n$ ($4 \leq n \leq 7$) electronic configuration may show a crossover between an LS and an HS state (Fig. 1). This crossover may be induced by variation of temperature or pressure, or by irradiation. To a first approximation, the crossover occurs when the enthalpy of the LS state in its equilibrium geometry is slightly lower than that of the HS state, also in its equilibrium geometry. At low temperature, the thermodynamically stable state is the LS state, of lowest enthalpy. On the other hand, when the temperature is higher than a certain temperature, denoted $T_{1/2}$, the HS state becomes the thermodynamically stable state, because the entropy associated with the HS state is much larger than the entropy associated with the LS state, and the $T\Delta S$ (tem-

perature multiplied by entropy) gain overcomes the enthalpy loss (17). $T_{1/2}$ is the temperature for which there is coexistence of 50% of LS and 50% of HS molecules. The most extensively studied spin-crossover compounds are those involving the Fe^{2+} ion with the $3d^6$ configuration (6). In octahedral surroundings, the 3d metal orbitals are split into the low-lying t_{2g} and high-lying e_g subsets. The LS state arises from the close-shell t_{2g}^6 electronic configuration and the HS state from the $t_{2g}^4 e_g^2$ electronic configuration. In the HS state, the anti-bonding e_g orbitals are doubly occupied, which results in a lengthening of the Fe-ligand bonds, compared with the LS state, typically by 0.15 to 0.18 Å (18, 19).

Polymeric Structures and Cooperativity

The fundamental origin of the spin-crossover phenomenon is molecular, but the shape of the temperature dependence of the high-spin molar fraction, $x_{\text{HS}} = f(T)$, depends strongly on intermolecular interactions. The more pronounced these intermolecular interactions are, the steeper the $x_{\text{HS}} = f(T)$ curve around $T_{1/2}$. When the magnitude of these intermolecular interactions overcomes a threshold value, the spin-crossover phenomenon may become cooperative. In such cases, we will speak of spin transition. The thermally induced transitions between LS and HS states may not only be very abrupt, but they may also occur with a hysteresis effect. In these cases, the temperature of the LS \rightarrow HS transition in the warming mode, $T_c \uparrow$, is higher than the temperature of the HS \rightarrow LS transition in the cooling mode, $T_c \downarrow$. The existence of hysteresis is of the utmost importance, because it confers a memory effect on the system. Between $T_c \uparrow$ and $T_c \downarrow$, the state of the system, LS or HS, depends on its history, and hence on the information which has been stored.

Numerous studies have been devoted to the origin of the cooperativity in spin-transition compounds, in particular by Gülich, Spiering, and co-workers (20-24). The cooperativity is associated with the fact that the equilibrium geometries in the LS and HS states are different. We are not focusing here on the theoretical aspect of the problem, but rather on how to design strongly cooperative

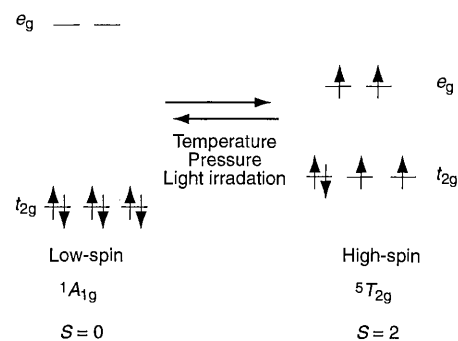


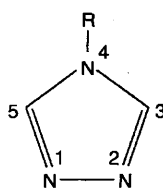
Fig. 1. LS and HS states for a molecular species formed by an Fe^{2+} ion surrounded by six ligands situated at the corners of an octahedron. At the molecular state, the spin-crossover corresponds to an intraionic transfer of two electrons between the t_{2g} and e_g orbitals, accompanied by a spin flip.

O. Kahn is in the Laboratoire des Sciences Moléculaires, Institut de Chimie de la Matière Condensée de Bordeaux, 33608 Pessac, France. C. J. Martinez is with the Delarue Card Systems, 14 rue Jean Baptiste Colbert, 14021 Caen, France.

*To whom correspondence should be addressed. E-mail: kahn@icmcb.u-bordeaux.fr

spin-transition compounds. The basic idea is the replacement of molecular crystals by polymers. In the former compounds, the active mononuclear species are located at the nodes of a crystal lattice, and the intermolecular interactions, predominantly van der Waals interactions, are weak. If the molecules are hydrogen-bonded, these interactions may be enhanced, but remain insufficient to give rise to a strong cooperativity. In the latter compounds, the active sites are linked to each other by chemical bridges through which the intersite interactions may be efficiently propagated. The first compound of this kind, of the formula $[\text{Fe}(\text{btrz})_2(\text{NCS})_2] \cdot \text{H}_2\text{O}$, was described in 1990 (25); in this compound, the active sites are bridged by the 4,4'-bis-1,2,4-triazole ligand (btrz), resulting in a two-dimensional structure. Very abrupt spin transitions, both in the warming and cooling modes, as well as a thermal hysteresis of 21 K were observed, with $T_c \uparrow = 144.5$ K and $T_c \downarrow = 123.5$ K. Moreover, the transition was accompanied by a well-pronounced change of color between violet (or pink) in the LS state and white in the HS state. The violet color results from the spin-allowed ${}^1A_{1g} \rightarrow {}^1T_{1g}$ d-d transition occurring at 520 nm; the white color arises from the fact that the spin-allowed d-d transition of lowest energy in the HS state, ${}^5T_{2g} \rightarrow {}^5E_g$, occurs in the near infrared. This marked change of color allows optical detection of the transition, by use of a set-up to record the transmittance of the material at 520 nm wavelength as a function of temperature (26).

In terms of applications for display devices, the ideal situation is obviously that where



Scheme 1

room temperature falls in the middle of the thermal hysteresis loop. We extensively explored the Fe^{2+} -4-R-1,2,4-triazole system, where 4-R-1,2,4-triazole (denoted hereafter as Rtrz) is the molecule shown below.

Most of the compounds we are concerned with have the general formula $[\text{Fe}(\text{Rtrz})_3]A_2 \cdot n\text{H}_2\text{O}$, where A^- is an anion and $n\text{H}_2\text{O}$ stands for noncoordinated water molecules. So far, no single crystal suitable for x-ray diffraction could be obtained. However, structural information has been deduced from EXAFS (x-ray absorption fine structure) at the iron K edge and from LAXS (large-angle x-ray scattering) spectra

(27–29). For all the compounds investigated so far, the structure in the LS state consists of linear chains in which the neighboring Fe atoms are triply bridged by Rtrz ligands through the N atoms occupying the 1- and 2-positions (Fig. 2). The shortest Fe-Fe separation is 3.65 Å, and the FeN_6 core is close to a regular octahedron. The alignment of the Fe atoms has been confirmed by the presence of a peak, both in EXAFS and LAXS spectra, characteristic of a Fe-Fe-Fe linear path. The chain structure is retained in the HS state, but it is not certain that the Fe atoms remain aligned. The peaks characteristic of a three-atom linear path disappeared. As expected, the average Fe-N bond is lengthened by 0.18 Å, and the FeN_6 core is distorted. Several crystal structures of the same type, with Cu replacing Fe^{2+} , were solved. All show linear chains of triply bridged metal ions (30). Linear trinuclear Fe^{2+} species in which the metal ions are triply bridged by 1,2,4-triazole ligands have also been characterized (31, 32).

Spin-Transition Regimes

Let us now focus on the types of spin transition encountered with the $[\text{Fe}(\text{Rtrz})_3]A_2 \cdot n\text{H}_2\text{O}$ compounds. All these compounds display the thermochromic effect already mentioned for $[\text{Fe}(\text{btrz})_2(\text{NCS})_2] \cdot \text{H}_2\text{O}$, and thus, the bistability can be detected optically. Four different types of spin transition may be distinguished:

1) The transitions are very abrupt with a well-shaped thermal hysteresis loop and a perfect reproducibility of this loop over successive thermal cycles. Such a behavior is rather rare. It has been observed so far for $[\text{Fe}(\text{NH}_2\text{trz})_3](\text{NO}_3)_2$ ($T_c \uparrow = 348$ K, $T_c \downarrow = 313$ K) (33, 34) and $[\text{Fe}(\text{Htrz})_2(\text{trz})](\text{BF}_4)$ ($T_c \uparrow = 383$ K, $T_c \downarrow = 345$ K) (35, 36). The chemical formula of this latter compound does not exactly correspond to the general formula given above; it contains an electron hole disordered over each $\text{Fe}(\text{Htrz})_2(\text{trz})\text{Fe}$ -bridging network.

2) The spin transitions are smoother, occurring over a range of at least 10 K, and the hysteresis width is in the range of 5 to 20 K. Many $[\text{Fe}(\text{Rtrz})_3]A_2 \cdot n\text{H}_2\text{O}$ compounds exhibit such behavior (37, 38), for instance, $[\text{Fe}(\text{NH}_2\text{trz})_3](\text{BF}_4)_2 \cdot \text{H}_2\text{O}$ with a hysteresis loop of 7 K centered at 255 K. Usually, the behavior is reproducible over successive thermal cycles. In such compounds, for a given Rtrz ligand, the transition temperatures decrease as the size of the anion A^- increases (39).

3) The observed behavior is governed by the synergy between spin transition and dehydration-rehydration process. This happens, for instance, for $[\text{Fe}(\text{NH}_2\text{trz})_3]$ -

$(\text{tosylate})_2 \cdot 2\text{H}_2\text{O}$ (40). At room temperature, the material is LS and has a violet color. As the temperature increases, the noncoordinated water molecules are removed, followed by an extremely abrupt transition at 361 K from the metastable LS state to the stable HS state of $[\text{Fe}(\text{NH}_2\text{trz})_3](\text{tosylate})_2$. The HS \rightarrow LS and LS \rightarrow HS transitions for the dehydrated compound $[\text{Fe}(\text{NH}_2\text{trz})_3](\text{tosylate})_2$ are smoother and occur at $T_c \downarrow = 279$ K and $T_c \uparrow = 296$ K. Usually, the dehydrated material is hygroscopic and spontaneously reverts to the starting material— $[\text{Fe}(\text{NH}_2\text{trz})_3](\text{tosylate})_2 \cdot 2\text{H}_2\text{O}$ in the chosen example—in a normal atmosphere at room temperature.

4) Some recently synthesized materials resemble those described in 3), with two important differences: the transitions for the dehydrated material occur at much lower temperature than for the hydrated one, and the dehydrated material is stable in normal conditions, that is, it does not reabsorb water. A typical example of such a behavior is offered by $[\text{Fe}(\text{hyettrz})_3]A_2 \cdot 3\text{H}_2\text{O}$ with $\text{hyettrz} = 4$ -(2'-hydroxy-ethyl)-1,2,4-triazole and $A^- = 3$ -nitro-phenylsulfonate (41). The LS \rightarrow HS transition for this compound is detected optically at 370 K, whereas the transition temperatures for the dehydrated material $[\text{Fe}(\text{hyettrz})_3]A_2$ are $T_c \downarrow = 100$ K and $T_c \uparrow = 110$ K (Fig. 3). In other words, once the starting violet material has turned white by heating, it remains white (and in the HS

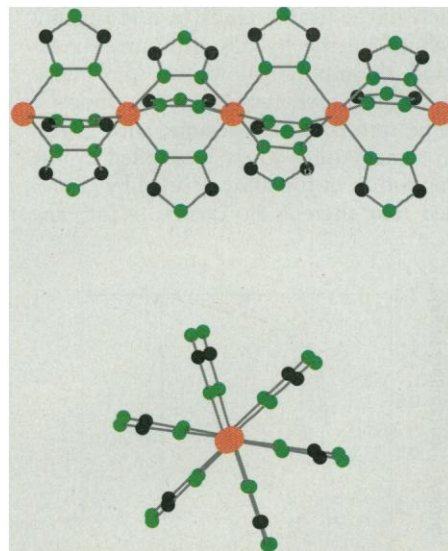


Fig. 2. Structure of a polymeric chain $[\text{Fe}(\text{Rtrz})_3]$ in the LS state of the spin-transition compounds $[\text{Fe}(\text{Rtrz})_3]A_2 \cdot n\text{H}_2\text{O}$, viewed both perpendicularly to (top) and along (bottom) the chain direction. For the sake of simplicity the R groups are omitted. They are bonded to the nitrogen atoms occupying the 4-positions of the triazole groups. The iron atoms are in red, the nitrogen atoms in green, and the carbon atoms in black.

state) when coming back to room temperature. We will discuss later the possible applications of such materials.

Molecular Alloys

The most appealing spin-transition materials in terms of active elements for display devices are those exhibiting behavior 1), provided that room temperature falls within the thermal hysteresis loop. So far, no pure material of this kind has been found. However, several approaches may be used to displace the thermal hysteresis loop. One possible approach is suggested by studies on doped spin-crossover compounds (34, 42–44). Replacing some Fe^{2+} ions by non-spin-crossover ions results in a decrease of the transition temperatures. This approach, however, has a drawback; the color contrasts between LS and HS states are less pronounced in doped materials than in pure compounds. A much more appealing approach has recently been proposed, which consists of designed molecular alloys. These alloys may be synthesized from two types of triazole ligands, R_1trz and R_2trz . Consider, for example, an alloy of the formula $[\text{Fe}(\text{R}_1\text{trz})_{3-3x}(\text{R}_2\text{trz})_{3x}]\text{A}_2 \cdot n\text{H}_2\text{O}$, constructed in such a way that along each chain there is a proportion $1-x$ of R_1trz ligands and x of R_2trz ligands. Such an alloy is obviously totally different from a mechanical mixture of two pure compounds $[\text{Fe}(\text{R}_1\text{trz})_3]\text{A}_2 \cdot n\text{H}_2\text{O}$ and $[\text{Fe}(\text{R}_2\text{trz})_3]\text{A}_2 \cdot n\text{H}_2\text{O}$ with the proportions $1-x$ and x , respectively. Such a mixture has $1-x$ chains in which all the ligands are R_1trz and x chains in which all the ligands are R_2trz . As expected, the mixture shows two spin-transition regimes, whereas the alloy shows a unique spin-transition regime, with transition temperatures solely controlled by the composition of the alloy defined by x , provided that there is no demixing into the

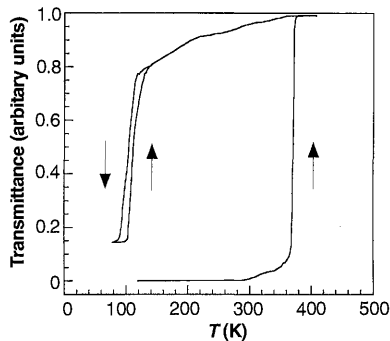


Fig. 3. Spin-transition behavior for the couple $[\text{Fe}(\text{hyetrz})_3]\text{A}_2 \cdot 3\text{H}_2\text{O} - [\text{Fe}(\text{hyetrz})_3]\text{A}_2$, with $\text{hyetrz} = 4-(2'-\text{hydroxy-ethyl})-1,2,4\text{-triazole}$ and $\text{A}^- = 3\text{-nitro-phenylsulfonate}$. The HS fraction was detected optically, through the transmittance of the material at 520 nm.

pure compounds. Such a behavior is displayed (Fig. 4) for the alloy $[\text{Fe}(\text{Htrz})_{3-3x}(\text{NH}_2\text{trz})_{3x}](\text{ClO}_4)_2 \cdot \text{H}_2\text{O}$. In that case, no demixing occurs, and $T_c \uparrow$ and $T_c \downarrow$ vary linearly as a function of x . Furthermore, the two ligands were chosen in such a way that the transition temperatures for one of the pure compounds are above room temperature, and for the other pure compound are below room temperature. It turns out that for a particular composition of the alloy, room temperature falls in the middle of the hysteresis loop. This material, with $x = 0.015$, is violet or white at room temperature depending on its history, or on the information which has been stored (45, 46).

This alloy behavior can be modeled in the framework of a mean-field description (47). We consider an alloy of composition A_aB_b , with $a + b = 1$, and define the HS molar fractions for the sites A and B as $x_{\text{HS}}(\text{A})$ and $x_{\text{HS}}(\text{B})$, respectively. What is experimentally detected, either magnetically or optically, is the total molar fraction of HS sites $x_{\text{HS}} = x_{\text{HS}}(\text{A}) + x_{\text{HS}}(\text{B})$. The Gibbs free energy of the alloy, G , is expressed as

$$G = G_{\text{LS}}(\text{A}) + G_{\text{HS}}(\text{A}) + G_{\text{LS}}(\text{B}) + G_{\text{HS}}(\text{B}) + G_{\text{exc}} - TS_{\text{mix}} \quad (1)$$

The first four terms on the right-hand side stand for the free energies of the A and B sites in both the LS and HS states; G_{exc} stands for the excess free energy arising from the intersite interactions AA, AB, and BB, and S_{mix} is the mixing entropy accounting for all the ways to distribute the A and B sites in LS and HS states in the lattice. The extrema of G are given by the solutions of

$$\partial G / \partial x_{\text{HS}}(\text{A}) = 0 \text{ and } \partial G / \partial x_{\text{HS}}(\text{B}) = 0 \quad (2)$$

which leads to a numerical solution $x_{\text{HS}} =$

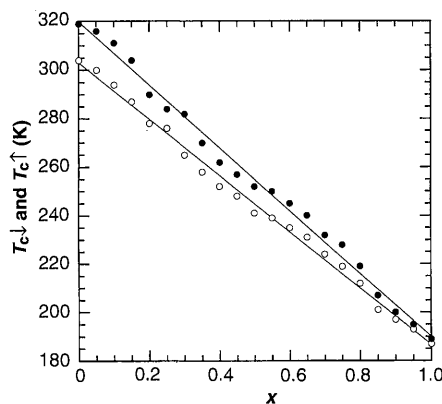


Fig. 4. Variation of the spin-transition temperatures $T_c \uparrow$ (●) and $T_c \downarrow$ (○) for the alloys $[\text{Fe}(\text{Htrz})_{3-3x}(\text{NH}_2\text{trz})_{3x}](\text{ClO}_4)_2 \cdot \text{H}_2\text{O}$ as a function of alloy composition.

$f(T)$. We will not detail further this calculation developed elsewhere (48), and will only present a typical result in Fig. 5. The $x_{\text{HS}} = f(T)$ curve for the $\text{A}_{0.5}\text{B}_{0.5}$ alloy is compared to both the curves for the two pure materials and the curve for the simple mixture of 50% of A and 50% of B. $T_{1/2}$ for the alloy occurs exactly halfway between the $T_{1/2}$ values for pure A and pure B. The curves of Fig. 5 also reveal a weakness of the molecular alloy approach; the transitions for the alloy are more gradual than for the pure compounds.

Another kind of alloy involves mixed counteranions instead of mixed triazole ligands. The spin-transition temperatures for a given type of cationic chains $[\text{Fe}(\text{Rtrz})_3]$ have been found to depend on the nature of the counteranion A, which suggests that the spin-transition regime may be also fine-tuned through the composition of alloys of the formula $[\text{Fe}(\text{Rtrz})_3]\text{A}_x\text{A}'_{1-x} \cdot n\text{H}_2\text{O}$. This possibility was tested for $\text{R} = \text{NH}_2$, $\text{A} = \text{NO}_3$, and $\text{A}' = \text{BF}_4$. Figure 6 shows the thermal hysteresis loop for the alloy $[\text{Fe}(\text{NH}_2\text{trz})_3](\text{NO}_3)_{1.7}(\text{BF}_4)_{0.3}$ preencapsulated in a polymer. The hysteresis loop has a width of about 60 K, and $T_c \uparrow$ and $T_c \downarrow$ are situated on either side of room temperature.

Design of Display Devices

The compounds described above exhibit both magnetic and optical changes when they undergo a spin transition. Their optical behavior is presently responsible for the

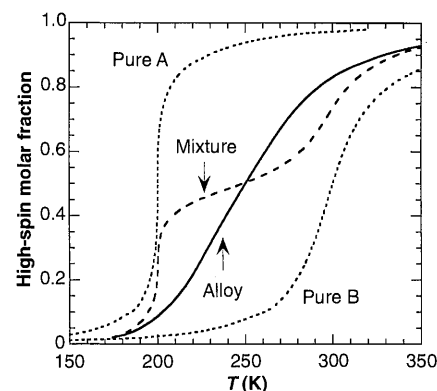


Fig. 5. Theoretical calculation in a mean-field approximation of the $x_{\text{HS}} = f(T)$ curve for the spin-transition molecular alloy $\text{A}_{0.5}\text{B}_{0.5}$. This curve is compared to those of the pure materials A and B, and that of a 50-50 mixture of A and B. The parameters of the calculations were chosen in such a way that $T_{1/2}$ is equal to 200 K for pure A and 300 K for pure B. The interaction parameter occurring in the excess free energy was taken equal to 278 cm^{-1} for all types of interaction (AA, BB, and AB). In this calculation, it was assumed that there were only two sites, A and B, but in the $[\text{Fe}(\text{R}_1\text{trz})_{3-3x}(\text{R}_2\text{trz})_{3x}]\text{A}_2 \cdot n\text{H}_2\text{O}$ compounds there are, of course, many more.

interest in their development. Two kinds of displays have already been investigated, involving type (iv) materials on the one hand and alloys working at room temperature on the other hand. In both cases, the writing step consists of locally warming up the display above $T_c \uparrow$. For a reversible display, the erasing step involves cooling down the material, locally or not, below $T_c \downarrow$, using for instance, a Peltier element. Such a reversible display is represented in Fig. 7.

The compounds of the type $[\text{Fe}(\text{hyettrz})_3] \text{A}_2 \cdot 3\text{H}_2\text{O}$ may be used as single-use displays, with a first level of security, because the materials cannot recover the hydrated LS state at room temperature without damage (mainly oxidation of Fe^{2+} ions). Such materials can indicate the first use of a prepaid stored-value card. They can also be used as temperature threshold indicators, because they can be designed in such a way that the transition temperature covers a range between -30°C and 100°C .

One of the main advantages of such displays is that they are easily implemented as a printed ink, deposited on any type of substrate such as plastic or paper. The design of the material then has to be completed by adjusting the ink basis, which mainly consists of a polymer solution. The ink basis has to comply with four criteria, namely: (i) to stick to the substrate, (ii) to be chemically neutral for the spin-transition material, (iii) to protect the material from environmental influences, and (iv) to be mechanically compatible with a printing principle of warming up. An intensive study led us to the choice of a screen-printing polymer basis with solvent subsequently evaporated.

The need for careful material design is even more pronounced with the second type

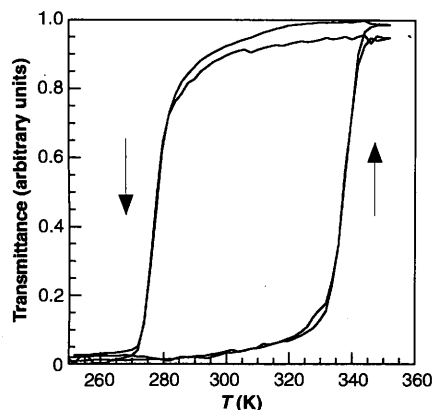


Fig. 6. Thermal hysteresis loop detected optically through the transmittance at 520 nm for the compound $[\text{Fe}(\text{NH}_2\text{trz})_3](\text{NO}_3)_{1.7}(\text{BF}_4)_{0.3}$ preencapsulated in a polymer. It has been checked that the hysteresis loop is reproducible over several dozen of thermal cycles. Two successive thermal cycles are represented here.

of displays, reversible ones, involving room-temperature working alloys. These alloys are sensitive to oxidation and humidity, and therefore preencapsulation of the material during the synthesis itself is required. Such a preencapsulation leads to hermetic, very thin, and transparent capsules around the spin-transition particles. Once this process is mastered, the resulting display is perfectly reversible, does not require any power supply to keep the message displayed, and is particularly easy to implement.

Alternative solutions are rather sparse. To the best of our knowledge, only two have been reported. One uses charged polyethylene terephthalate, where the charge undergoes local nucleation and denucleation, depending on the thermal treatment applied (warming up for both nucleation and denucleation, but at different temperatures), thus leading to diffusive or transparent states, respectively. The system suffers from fatigue during successive cycles. The second one involves magnetic particles that are oriented perpendicular or parallel to the substrate. To work, it requires a dedicated substrate, which is not always compatible with a

cost target. This technique remains highly sensitive to interferences with residual magnetic fields.

Further Perspectives

Spin-transition polymers exhibit some fundamental features such as magnetic and optical transitions, and bistability that make them relevant for further investigation as storage media. The increasing importance of electronic data retrieval and storage reveals a need, and in the meantime a challenge, for high-density storage media. Within the last 40 years, the bit length has decreased from 250 μm (the first hard disk from IBM in 1950) to 1 μm in audio compact discs and even 0.6 μm (compare work on frequency-doubling systems by IBM in 1994). These reductions in size have taken place in parallel with the emergence of higher data transfer rates (the typical range is currently 9 megabits per second) and shorter information access times, typically 30 ms. Whereas the latter figure is exclusively linked to the reading process, the other two parameters

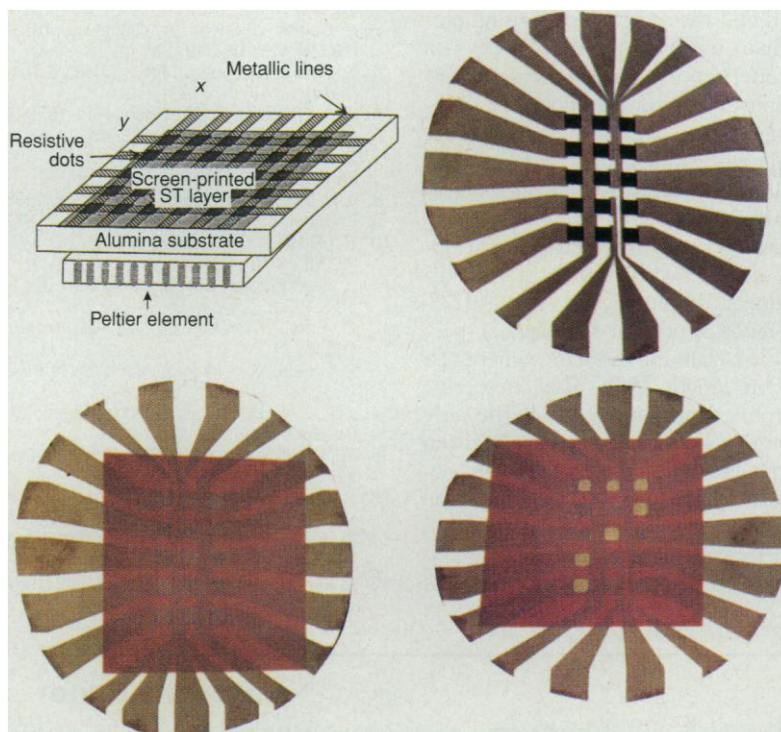


Fig. 7. Principles of a display using a spin-transition polymer as active element. The substrate consists of an alumina plate, on which resistive dots and connecting electrodes were previously screen printed. The dots are addressed through columns and rows. The addressing step can be monitored through a computer (top). A layer of the active material is deposited on the substrate. This is done by screen-printing technology, using an ink consisting of the material in suspension in a resin which acts as both a material support and a protection against the environment (bottom left). The dots, when electrically addressed, act as heat dissipators. When the temperature is above $T_c \uparrow$, the material passes from violet to white. The information is stored as long as the system remains at a temperature within the hysteresis loop (bottom right). To erase, the temperature has to be lowered below $T_c \downarrow$. This can be achieved with a Peltier element. Various related displays can be derived from the one shown in this figure.

are directly related to the material itself and to the storage process.

To further increase the integration, even with existing writing tools (the predicted limit for optical writing is a density of 100 bits per square micrometer), there is a crucial need for new materials. Spin-transition polymers have already offered interesting capabilities such as: (i) room-temperature working range, (ii) wide thermal hysteresis loops (50 K and more), (iii) low thermal addressing power (about 5×10^{-2} mW/ μm^2), (iv) short addressing time (the intrinsic time scale of the phenomenon is of the order of nanoseconds), and (v) very small bit size. Regarding this last point, the minimum size for one bit is not one repeat unit $[\text{Fe}(\text{Rtrz})_3]$, but the smallest particle that exhibits cooperativity. It has been estimated that about 10^3 strongly interacting active sites should exhibit a cooperative behavior. This roughly corresponds to a cube of 4 nm per edge and potentially represents a decrease by two orders of magnitude in the characteristic bit size. Note that a single-electron transistor has been reported by researchers at the University of Minnesota, with a characteristic gate size of 6 nm (49). With such a degree of miniaturization, the implementation of the compound and the writing and erasing processes remain unsolved problems. This is a general concern for high-density data storage. For spin-transition materials, the Langmuir-Blodgett film approach has been the first to be investigated. It may lead to regular bidimensional media, with controlled densities of active sites (50).

Concerning the writing-erasing and reading tools, at least two high-definition methods are under development. Both AT&T and IBM reported on near-field optical spectroscopy (51), claiming the achievement of a 0.06- μm bit length (52). The alternative route is atomic force microscopy. In the early 1990s, the first thermomechanically written bits on polymethylmethacrylate were obtained, with lengths of 120 nm (53). The best performances are around 3- to 6-nm bits, even though the accuracy of this technique is not on the atomic scale. As far as

spin-transition materials are concerned, thermal writing has already proved its applicability. Nevertheless, localized erasure remains difficult to achieve.

Up to now, we focused on the optical properties of the materials in terms of applications. We would like to mention another kind of temperature sensor whose response is not provided by the color, but by the magnetic properties. In magnetic resonance imaging, it may be important to know the in situ temperature or to receive an alert when an upper-limit temperature is reached. For instance, this is the case for the treatment of some tumors by hyperthermy. A compound designed in such a way that its transition temperature corresponds to this upper-limit temperature may be used. Below this temperature, the compound is diamagnetic, and the magnetic resonance image is not perturbed. When the critical temperature is reached, the compound becomes paramagnetic, and the magnetic resonance image is strongly perturbed.

REFERENCES

1. O. Kahn and J. P. Launay, *Chemtronics* **3**, 140 (1988).
2. L. Cambi and A. Gagnasso, *Atti. Accad. Naz. Lincei* **13**, 809 (1931).
3. L. Cambi, L. Szegö, A. Gagnasso, *ibid.* **15**, 266 (1932a); *ibid.* **15**, 329 (1932b).
4. S. Sorai and S. Seki, *J. Phys. Chem. Solids* **35**, 555 (1974).
5. H. A. Goodwin, *Coord. Chem. Rev.* **18**, 293 (1976).
6. P. Güttlich, *Struct. Bonding (Berlin)* **44**, 83 (1981).
7. E. König, G. Ritter, S. K. Kulshreshtha, *Chem. Rev.* **85**, 219 (1985).
8. J. K. Beattie, *Adv. Inorg. Chem.* **32**, 1 (1988).
9. E. König, *Struct. Bonding (Berlin)* **76**, 51 (1991).
10. P. Güttlich and A. Hauser, *Coord. Chem. Rev.* **97**, 1 (1990).
11. J. Zarembowitch and O. Kahn, *New J. Chem.* **15**, 181 (1991).
12. O. Kahn, J. Kröber, C. Jay, *Adv. Mater.* **4**, 718 (1992).
13. P. Güttlich, *Nucl. Instrum. Methods Phys. Res. B* **76**, 387 (1993).
14. ———, A. Hauser, H. Spiering, *Angew. Chem. Int. Ed. Engl.* **33**, 2024 (1994).
15. S. Decurtins, P. Güttlich, C. P. Köhler, H. Spiering, A. Hauser, *Chem. Phys. Lett.* **104**, 1 (1984).
16. S. Decurtins, P. Güttlich, K. M. Hasselbach, A. Hauser, H. Spiering, *Inorg. Chem.* **24**, 2174 (1985).
17. O. Kahn, *Molecular Magnetism* (VCH, New York, 1993).
18. E. König, *Prog. Inorg. Chem.* **35**, 527 (1987).
19. B. Gallois, J. A. Real, C. Hauw, J. Zarembowitch, *Inorg. Chem.* **29**, 1152 (1990).
20. N. Sasaki and T. Kambara, *J. Phys. Soc. Jpn.* **49**, 1806 (1987).
21. H. Spiering, E. Meissner, H. Köppen, E. W. Müller, P. Güttlich, *Chem. Phys.* **68**, 65 (1982).
22. ———, *J. Phys. Chem. Solids* **48**, 517 (1987).
23. H. Spiering and N. Willenbacher, *J. Phys. Condens. Matter* **1**, 10089 (1989).
24. H. Bolvin and O. Kahn, *Chem. Phys.* **192**, 295 (1995).
25. W. Wreugdenhil *et al.*, *Polyhedron* **9**, 2971 (1990).
26. O. Kahn and E. Codjovi, *Philos. Trans. R. Soc. London Ser. A* **354**, 359 (1996).
27. A. Michalowicz, J. Moscovič, B. Ducourant, D. Cracco, O. Kahn, *Chem. Mater.* **7**, 1833 (1995).
28. A. Michalowicz, J. Moscovič, O. Kahn, *J. Phys. IV (Paris)* **7**, C2-633 (1997).
29. M. Verelst, unpublished observations.
30. G. Vos *et al.*, *Inorg. Chem.* **23**, 2905 (1984).
31. V. P. Sinditskii *et al.*, *Russ. J. Inorg. Chem.* **32**, 1149 (1987).
32. M. Thomann, O. Kahn, J. Guilhem, F. Varret, *Inorg. Chem.* **33**, 6029 (1994).
33. L. G. Lavrenova, V. N. Ikorskii, V. A. Varnek, I. M. Oglezneva, S. V. Larionov, *Koord. Khim.* **12**, 207 (1986).
34. ———, *J. Struct. Chem.* **34**, 960 (1993).
35. K. H. Sugiyarto and H. A. Goodwin, *Aust. J. Chem.* **47**, 263 (1994).
36. J. Kröber *et al.*, *Chem. Mater.* **6**, 1404 (1994).
37. L. G. Lavrenova, V. N. Ikorskii, V. A. Varnek, I. M. Oglezneva, S. V. Larionov, *Koord. Khim.* **16**, 654 (1990).
38. L. G. Lavrenova *et al.*, *Polyhedron*, **14**, 1333 (1995).
39. V. A. Varnek and L. G. Lavrenova, *J. Struct. Chem.* **36**, 104 (1995).
40. E. Codjovi, L. Sommier, O. Kahn, C. Jay, *New J. Chem.* **20**, 503 (1996).
41. Y. Garcia *et al.*, *J. Mater. Chem.* **7**, 857 (1997).
42. P. Ganguli, P. Güttlich, E. W. Müller, *Inorg. Chem.* **21**, 3439 (1982).
43. I. Sanner, E. Meissner, H. Köppen, H. Spiering, P. Güttlich, *Chem. Phys.* **86**, 227 (1984).
44. J. P. Martin, J. Zarembowitch, A. Dworkin, J. G. Haasnoot, E. Codjovi, *Inorg. Chem.* **33**, 2617 (1994).
45. O. Kahn *et al.*, in *Molecule-Based Magnetic Materials*, Symposium Series No. 644, M. M. Turnbull, T. Sugimoto, L. K. Thompson, Eds. (American Chemical Society, Washington, DC, 1996), p. 298.
46. J. Kröber, E. Codjovi, O. Kahn, F. Grolière, C. Jay, *J. Am. Chem. Soc.* **115**, 9810 (1993).
47. C. P. Schlichter and H. G. Drickamer, *J. Chem. Phys.* **56**, 2142 (1972).
48. O. Kahn, L. Sommier, E. Codjovi, *Chem. Mater.*, in press.
49. *Electron. Des.* **45** (no. 7), 29 (1997).
50. P. Coronel *et al.* *J. Chem. Soc. Chem. Commun.* **1989**, 193 (1989).
51. B. D. Terris, H. J. Mamin, D. Rugar, *Appl. Phys. Lett.* **68**, 141 (1996).
52. E. Betzig *et al.*, *AT&T News Release*, 5 August 1992.
53. H. J. Mamin and D. Rugar, *Appl. Phys. Lett.* **61**, 1003 (1992).

Associate Editor

An editorial position at SCIENCE is available for a Ph.D. scientist in physics with a strong background in condensed-matter physics, spectroscopy, or optics. We are seeking a candidate with two or more years of postdoctoral experience who has published in the peer-reviewed literature. Responsibilities include selection and editing of manuscripts, assistance with solicitation of review and commentary pieces, and maintaining contact with the scientific community at meetings and laboratories. Previous editorial experience is not required. This is a full-time regular position in either our Washington, D.C., office or our Cambridge, U.K., office.

Please submit cover letter, resume, and salary requirements to:

The American Association for the Advancement of Science
Human Resources Department
Suite #100, AE-1213
1200 New York Avenue, NW
Washington, DC 20005

Equal Opportunity Employer and Nonsmoking work environment.